Available online at www.worldscientificnews.com

World Scientific News

An International Scientific Journal

WSN 155 (2021) 1-22 EISSN 2392-2192

Combined effects of thermal radiation and Hall current on MHD Casson nanofluid exerted by peristaltic transport

S. K. Asha[1,*] and **Chandrashekhar Hadapad**[2]

Department of Mathematics, Karnatak University, Pavate Nagar, Dharwad 580003, India

[1,2]E-mail address: as.kotnur2008@gmail.com , chandruh.h4@gmail.com

ABSTRACT

The present work intends to analyse the MHD Casson nano fluid inside an asymmetric channel. The equations governing the fluid flow admit both Thermophoresis and Brownian motion alongside thermal radiation. We acquired closed form analytical solutions for temperature, axial velocity, nanoparticle concentration and pressure gradient profiles. The ascendency of governing parameters like thermal radiation parameter, thermophoresis, Brownian, Hartmann number and Hall parameter on dimensionless temperature, concentration and pressure gradient profiles have been explained in detailed manner with the aid of plots and table. The prevailed results in this article are verified with prior available literature for specific cases and they are in good agreement.

***Keywords*:** thermal radiation, nanofluid, MHD, Hall current, peristaltic transport

1. INTRODUCTION

The stereotyped heat transfer fluids (HTF) like ethylene glycol, oil and water, shows an intrinsic property of poor thermal behaviour. Because of their low thermal capabilities in heat transfer phenomena there is an advantage for metals and non-metals like copper, silver, SiC, Cuo shows improvised and ultra-high thermal conductivities in comparison with traditional heat

(Received 07 February 2021; Accepted 27 February 2021; Date of Publication 28 February 2021)

transfer fluids (HTF). An offbeat idea of immersing solid materials in base fluids to overcome the limitation of HTFs in showing low capabilities of heat transfer was initiated by Maxwell [1]. The idea of using small 10^{-3} or 10^{-6} meter sized solid particles, provided a route to issues like rapid settling in fluids, jamming in micro tubes, laceration of surface and also the high pressure descent which restricted them in practical applications. The present area nanotechnology furnished an opportunity to process and make particles with standard opaque sizes less than 50 nanometre which brings in base fluids an enhanced thermal behaviour in lowering substantial heat loss in heating and cooling processes.

Choi [2] had come up with fresh idea of nano-fluids by incorporating these materials which are ranges from 1-100 nm. The term nano-fluids were originated by Choi and Eastman [3]. These fluids refers to a kind of nanotechnology oriented heat transfer fluids made by immersing mili-micron sized materials inside traditional heat transfer fluids also with a substance which tends to reduce the surface tension of a fluid to enhance stability in thermal conduction usually the oxides of metals, nitrides, carbon ceramics, semiconductors, nitrides etc. are used as nanoparticles.

Vassalo et al. [4] and You et al. [5] brought out some of the work related to fact that thermal capabilities in heat transfer processes are more improved for nano-fluids contrast to orthodox fluids. They have established that immersing less amount of nanoparticles to ordinary fluids payoff advancement in the conduction capabilities of the fluids. For further reading see refs [6-10].

In commercial applications where requirements regarding rate of cooling cannot be fulfilled by the normal heat conductive fluids due to their ineffective thermal conductivity, it can be enhanced by the application of nanoparticles wherein Brownian motion of the particle increases the capabilities which helps in thermal conductivity. Moreover the Magneto-hydrodynamic (MHD) nanofluids display a vital role in these applications. These fluids can be widely employed in modulating processes; filters which use fibres, switches, in cooling process etc. for further reading refer these [11-15].

The classification of non-Newtonian behaviour whose viscidity declines under shear strain is the casson fluid model. This is a shear-thinning or pseudoplastic fluid in which observable fluid viscosity diminishes with increased stress. The best suited example for shear thinning fluid is human blood as it permits the blood viscosity to decline when there is a rise in rate of shear strain.

Similar behaviour can be seen in materials like paint, sand in water, ketchup, soup, honey etc. this fluid model behaves like a kind of a flexible solid beyond a threshold shear stress and low shear strain. At a negligibly small rate of stress this fluid has an infinite viscidity, but the viscosity reduces to zero when raised to an infinite shear stress. For more refs [16-22].

Thermal conduction or convection flows strengthened the need of thermal radiation in day to day biomedical applications such as IR (Infrared Radiation) in treating various parts of the human body.

In compliance with the fact that radiative energy transfer does not require any intervening medium for radiant exchange between two body and also its dependency over the absolute temperature differences, radiation effect can be seen substantially in many applications like in power plants, Engines, measuring the thermal effects in Rocket nozzles, some technology incuding the utililization of solar energy radiation etc. for further reading see refs [23-28].

We have used Rosseland's approximation for linearization of thermal radiation.

2. PROBLEM FORMULATION

Consider a viscous, incompressible, steady two dimensional peristaltic motion of Casson nanofluid model in an asymmetric channel of fixed thickness $d_2 + d_1$. The fluid motion inside the walls is fabricated by propagation of sinusoidal waves of less amplitudes a_1 and b_1 with steady speed c of the channel walls. The mathematical description of the geometry of the conduit (Figure 1) can be written as

$$\dot{Y} = \dot{h}_1 = a_1 Cos\left(\left[\dot{X} - c\dot{t}\right]\frac{2\pi}{\lambda}\right) + d_1, \tag{1}$$

$$\dot{Y} = \dot{h}_2 = -a_2 Cos\left(\left[\dot{X} - c\dot{t}\right]\frac{2\pi}{\lambda} + \dot{\phi}\right) - d_2, \tag{2}$$

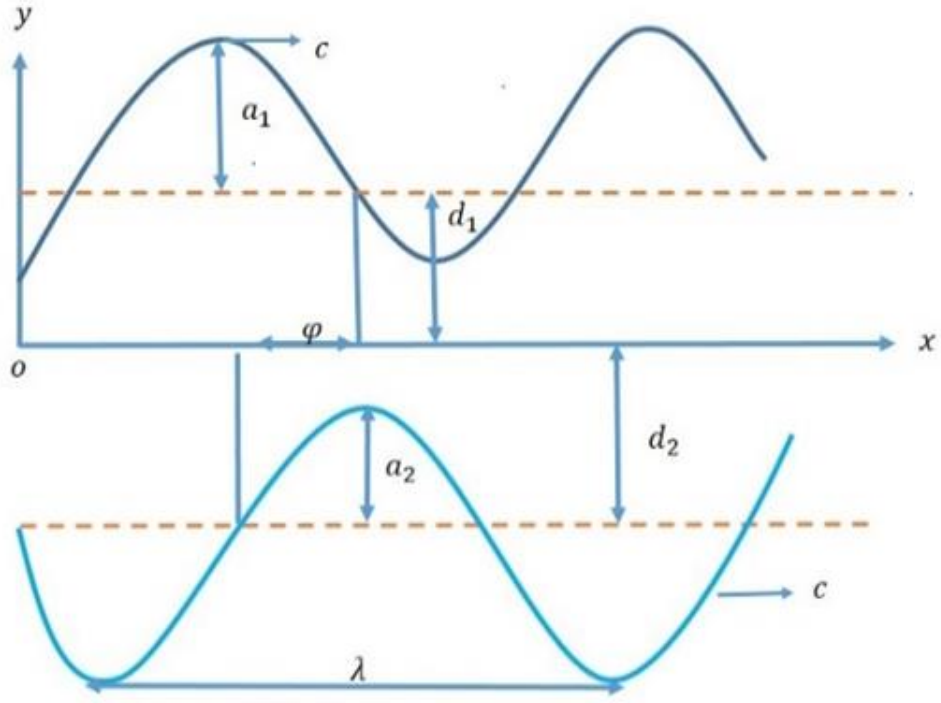

Figure 1. Schematic diagram of physical model

We have assumed Cartesian co-ordinate system $(\dot{X}, \dot{Y})$ where $\dot{X}$ and $\dot{Y}$ are perpendicular to one another, λ is the wavelength, $\dot{t}$ is the time, $\dot{\phi}$ is the phase difference and with d_1 and d_2 satisfying the condition:

$$a_1^2 + b_1^2 + 2a_1 b_1 Cos\,\dot{\phi} \le d_1^2 + d_2^2. \tag{3}$$

Which helps in keeping the walls not intersecting each other. The effect of uniform applied magnetic field with density vector $B=(0,0,B_0)$ can be neglected if it is assumed to be low Reynolds number. The equation for J (current density) comprising the Hall effect, ion slip, and thermoelectric is given by Ref [29].

$$J=\sigma\left[E+\dot{V}\times B-(J\times B)\frac{1}{e\,n_e}\right], \tag{4}$$

$$J\times B=\frac{\sigma B_0^2}{1+m^2}\left[(\dot{U}+m\dot{V}),\,(m\dot{U}-\dot{V}),\,O\right]. \tag{5}$$

where J is the current density, σ is the electric conductivity of the fluid, $\dot{U}$ and $\dot{V}$ are the coordinates of the velocity and $m=\frac{e\,B_0}{e\,n_e}$ is the Hall term. We have considered that $E=0$ (no applied voltage), e is the electric charge and n_e is the electron density.

Velocity $\dot{V}$ in vector form can be written as,

$$\dot{V}=(\dot{U}(\dot{X},\dot{Y},\dot{t}),\dot{V}(\dot{X},\dot{Y},\dot{t})) \tag{6}$$

where $\dot{U}(\dot{X},\dot{Y},\dot{t})$ and $\dot{V}(\dot{X},\dot{Y},\dot{t})$ are the velocity field components.

The Constitutive equation of a Casson fluid model is

$$\tau_{ij}=(\mu_0+\frac{\rho_y}{\sqrt{2\pi_c}})2e_{ij},\quad \text{When}\quad \pi<\pi_c, \tag{7}$$

$$\tau_{ij}=(\mu_0+\frac{\rho_y}{\sqrt{2\pi_c}})2e_{ij},\quad \text{When}\quad \pi>\pi_c. \tag{8}$$

where $\rho_y=\frac{\mu_0\sqrt{2\pi}}{\beta}$, the yield stress of the fluid is, μ_0 is the plastic dynamic viscosity of the non-Newtonian fluid, π is the product of the component of the rate of deformation with itself. (i.e. $\pi=e_{ij}.e_{ij}$), e_{ij} - $(i,j)^{th}$ component of the rate of deformation and π_c is the critical value based on the non-Newtonian model.

The radiative heat flux in accordance with Rosseland's approximation [29], $\dot{q}_r$ can be modelled as

$$\dot{q}_r=-16\frac{\dot{\sigma}\dot{T}_1^3}{3\dot{k}}\frac{\partial\dot{T}}{\partial y}. \tag{9}$$

where $\dot{k}$ denotes the Rosseland mean absorption, and $\dot{\sigma}$ is the Stefan –Boltzmann constant.

The governing equations portraying the peristaltic motion of a two dimensional steady Casson nanofluids are as follows.

$$\frac{\partial \dot{U}}{\partial \dot{X}}+\frac{\partial \dot{V}}{\partial \dot{Y}}=0 \tag{10}$$

$$\rho\left[\frac{\partial \dot{U}}{\partial \dot{t}}+\dot{U}\frac{\partial \dot{U}}{\partial \dot{X}}+\dot{V}\frac{\partial \dot{U}}{\partial \dot{Y}}\right]=-\frac{\partial \dot{P}}{\partial \dot{x}}+\mu\left(1+\frac{1}{\beta}\right)\left(\frac{\partial^2 \dot{U}}{\partial \dot{X}^2}+\frac{\partial^2 \dot{U}}{\partial \dot{Y}^2}\right)+\frac{\sigma B_0^2}{1+m^2}\dot{U}+\rho g B_r(\dot{T}-\dot{T}_0)+\rho g B_c(\dot{C}-\dot{C}_0), \tag{11}$$

$$\rho\left[\frac{\partial \dot{V}}{\partial \dot{t}}+\dot{U}\frac{\partial \dot{V}}{\partial \dot{X}}+\dot{V}\frac{\partial \dot{V}}{\partial \dot{Y}}\right]=-\frac{\partial \dot{P}}{\partial \dot{Y}}+\mu\left(1+\frac{1}{\beta}\right)\left(\frac{\partial^2 \dot{V}}{\partial \dot{X}^2}+\frac{\partial^2 \dot{V}}{\partial \dot{Y}^2}\right)-\frac{\sigma B_0^2}{1+m^2}\dot{V}, \tag{12}$$

$$\begin{aligned}(\rho c)_t\left[\frac{\partial \dot{T}}{\partial \dot{t}}+\dot{U}\frac{\partial \dot{T}}{\partial \dot{X}}+\dot{V}\frac{\partial \dot{T}}{\partial \dot{Y}}\right]&=k_T\left(\frac{\partial^2 \dot{T}}{\partial \dot{X}^2}+\frac{\partial^2 \dot{T}}{\partial \dot{Y}^2}\right)+(\rho c)_p\frac{D_T}{D_m}\left(\left(\frac{\partial \dot{T}}{\partial \dot{X}}\right)^2+\left(\frac{\partial \dot{T}}{\partial \dot{Y}}\right)^2\right)\\&+(\rho c)_p\left[D_B\left(\frac{\partial \dot{C}}{\partial \dot{X}}\frac{\partial \dot{T}}{\partial \dot{X}}+\frac{\partial \dot{C}}{\partial \dot{Y}}\frac{\partial \dot{T}}{\partial \dot{Y}}\right)\right]-\frac{\partial \dot{q}_r}{\partial \dot{Y}}\end{aligned} \tag{13}$$

$$\frac{\partial \dot{C}}{\partial \dot{t}}+\dot{U}\frac{\partial \dot{C}}{\partial \dot{X}}+\dot{V}\frac{\partial \dot{C}}{\partial \dot{Y}}=D_B\left(\frac{\partial^2 \dot{C}}{\partial \dot{X}^2}+\frac{\partial^2 \dot{C}}{\partial \dot{Y}^2}\right)+\frac{D_T}{D_m}\left(\frac{\partial^2 \dot{T}}{\partial \dot{X}^2}+\frac{\partial^2 \dot{T}}{\partial \dot{Y}^2}\right). \tag{14}$$

where $\dot{U}$ and $\dot{V}$ are the components of velocity in $\dot{X}$ and $\dot{Y}$ axes being perpendicular to each other. Pressure $\dot{P}$, Hall term m, temperature distribution $\dot{T}$, ρ_p is the base fluid density, Electrical conductivity of the fluid σ, coefficient of volumetric expansion β, strength of the applied magnetic field B_0, k_T is the thermal conductivity of the fluid, reference temperature $\dot{T}_1$, concentration $\dot{C}$, $(\rho c)_p$ is the nanoparticles effective heat capacity, D_T is the coefficient of thermophoresis diffusion, D_B coefficient of Brownian diffusion, T_m mean fluid temperature, $\dot{q}_r$ radiative heat flux, $\dot{T}$ is the temperature of the fluid, q is the gravity.

The corresponding dimensional boundary conditions are

$$\dot{U}=-c,\ \dot{T}=\dot{T}_0,\dot{C}=\dot{C}_0,\ \text{at}\quad \dot{Y}=\dot{h}_1=d_1+a_1Cos\left(\left(\dot{X}-c\dot{t}\right)\frac{2\pi}{\lambda}\right),$$

$$\dot{U}=-c,\ \dot{T}=\dot{T}_1,\dot{C}=\dot{C}_1,\ \text{at}\quad \dot{Y}=\dot{h}_2=-d_2-b_1Cos\left(\left(\dot{X}-c\dot{t}\right)\frac{2\pi}{\lambda}+\dot{\phi}\right). \tag{15}$$

Relation between wave frame and lab frame are established by

$$\dot{x}=\dot{X}-c\dot{t},\ \dot{u}=\dot{U}-c,\ \dot{y}=\dot{Y},\ \dot{v}=\dot{V}. \tag{16}$$

The dimensionless parameters are

$$\left.\begin{aligned}
&x=\frac{\dot{X}}{\lambda},\ y=\frac{\dot{Y}}{d_1},\ t=\frac{c\dot{t}}{\lambda},\ \delta=\frac{d_1}{\lambda},\ d=\frac{d_2}{d_1},\ u=\frac{\dot{U}}{c},\ M=\sqrt{\frac{\sigma}{\mu}}B_0d_1,\ a=\frac{a_1}{d_1},\psi=\frac{\dot{\psi}}{cd_1},\\
&\theta=\frac{\dot{T}-\dot{T}_0}{\dot{T}_1-\dot{T}_0},\ c=\frac{\dot{C}-\dot{C}_0}{\dot{C}_1-\dot{C}_0},\ h_2=\frac{\dot{h}_2}{d_2},\ h_1=\frac{\dot{h}_1}{d_1},\ v=\frac{\dot{V}}{c},\ b=\frac{b_1}{d_1},\ \mathrm{Pr}=\frac{\mu C_f}{\alpha},\ \alpha=\frac{k}{(\rho c)_f},\\
&Rd=\frac{16\dot{\sigma}\dot{T}_1^{\,3}}{3\dot{k}},\ Re=\frac{\rho c d_1}{\mu},\ N_b=\frac{(\rho c)_p(\dot{C}_1-\dot{C}_0)\mathrm{D}_B}{(\rho c)_f\ \nu},\ N_t=\frac{(\rho c)_p(\dot{T}_1-\dot{T}_0)\mathrm{D}_T}{(\rho c)_f\ T_m},\\
&G_r=\frac{gld_1^{\,3}(\dot{T}_1-\dot{T}_0)}{\mu c},\ B_r=\frac{gld_1^{\,3}(\dot{C}_1-\dot{C}_0)}{\mu c},\ u=\frac{\partial\psi}{\partial y},v=-\delta\frac{\partial\psi}{\partial x}.
\end{aligned}\right\} \tag{17}$$

In view of (17) equations (11)-(14), reduces to

$$\frac{\partial p}{\partial x}-\left(1+\frac{1}{\beta}\right)\frac{\partial^2u}{\partial y^2}+\frac{M^2}{1+m^2}u-G_r\theta-B_r\Omega=0, \tag{18}$$

$$\frac{\partial p}{\partial y}=0, \tag{19}$$

$$\frac{\partial^2\theta}{\partial y^2}+N_tPr\left(\frac{\partial\theta}{\partial y}\right)^2+N_bPr\frac{\partial\theta}{\partial y}\frac{\partial\Omega}{\partial y}+Rd\,Pr\frac{\partial^2\theta}{\partial y^2}=0, \tag{20}$$

$$\frac{\partial^2\Omega}{\partial y^2}+\frac{N_t}{N_b}\frac{\partial^2\theta}{\partial y^2}=0. \tag{21}$$

The dimensionless boundary conditions are

$$u = -1,\ C = 0, \theta = 0 \quad at\ \ y = h_1, \tag{22}$$

$$u = -1,\ C = 1, \theta = 1 \quad at\ \ y = h_2, \tag{23}$$

3. CLOSED FORM OF SOLUTION

Integrating once equation (21), we get

$$\frac{\partial \Omega}{\partial y} = -\frac{N_t}{N_b}\frac{\partial \theta}{\partial y} + C_1, \tag{24}$$

Substituting equation (24) in equation (20) and after simplification we get,

$$\frac{\partial^2 \theta}{\partial y^2} = A\frac{\partial \theta}{\partial y}. \tag{25}$$

Implementing Adomian decomposition method for equation (25) gives

$$\theta = C_3 + C_4 y + L_{yy}^{-1}\left\{A\frac{\partial \theta}{\partial y}\right\},$$

Now,

$$\theta_0 = C_3 + C_4 y,$$
$$\theta_{n+1} = A L_{yy}^{-1}\left\{\frac{\partial \theta_n}{\partial y}\right\},\ n \geq 0. \tag{26}$$

Following equation (26) we get,

$$\left.\begin{aligned}
\theta_1 &= AC_4\frac{y^2}{2!} \\
\theta_2 &= A^2 C_4\frac{y^3}{3!} \\
\theta_3 &= A^3 C_4\frac{y^4}{4!} \\
\theta_4 &= A^4 C_4\frac{y^5}{5!}
\end{aligned}\right\}$$

and so on.

Decomposition of θ as $\theta = \sum_{n=0}^{\infty} \theta_n.$ gives,

$$\theta = C_3 + \frac{C_4}{A}\left[\left\{Ay + \frac{(Ay)^3}{3!} + \frac{(Ay)^5}{5!} + --\right\} + \left\{\frac{(Ay)^2}{2!} + \frac{(Ay)^4}{4!} + \frac{(Ay)^4}{4!} --\right\}\right],$$

i.e., $\theta = C_3 + \frac{C_4}{A}\left(SinhAy + CoshAy\right).$ (27)

Integrating once again equation (24) we get

$$\Omega = -\frac{N_t}{N_b}\theta + C_1 y + C_2. \quad (28)$$

Substituting equation (27) in above equation (28) for Ω ,

$$\Omega = -\frac{N_t}{N_b}\left\{C_3 + \frac{C_4}{A}\left(SinhAy + CoshAy\right)\right\} + C_1 y + C_2. \quad (29)$$

Equation (18) can be rewritten as

$$L_{yy}u - N^2 u = \left\{A_0\frac{\partial p}{\partial x} - B_0\theta - C_0\Omega\right\}, \quad (30)$$

where L_{yy} being a differential operator of second order, so L_{yy}^{-1} is a inverse second order integration operator defined by

$$L_{yy}^{-1}(.) = \int_0^y \int_0^y (.)\, dydy. \quad (31)$$

Operating with L_{yy}^{-1}, equation (24) becomes

$$u = C_5 + C_6 y + L_{yy}^{-1}\left\{A_0\frac{\partial p}{\partial x}\right\} - L_{yy}^{-1}\left\{B_0\,\theta\right\} - L_{yy}^{-1}\left\{C_0\,\Omega\right\} + N^2 u. \quad (32)$$

Equation (26) gives,

$$u_0 = C_5 + \frac{C_6}{N}(Ny) + \frac{A_0}{N^2}\frac{\partial p}{\partial x}\left\{\frac{(Ny)^2}{2!}\right\} - \frac{B_0}{A^2 F_1}\left(SinhAy + CoshAy\right) + \frac{B_0 F_0}{N^2 F_1}\left\{\frac{(Ny)^2}{2!}\right\}$$
$$- \frac{C_0 N_t F_0}{N_b N^2 F_1}\left\{\frac{(Ny)^2}{2!}\right\} + \frac{C_0 N_t}{N_b A^2 F_1}\left(SinhAy + CoshAy\right) - \frac{C_0(N_t + N_b)}{N_b N^3 (h_2 - h_1)}\left\{\frac{(Ny)^3}{3!}\right\}$$
$$+ \frac{C_0(N_t + N_b)h_1}{N_b N^2 (h_2 - h_1)}\left\{\frac{(Ny)^2}{2!}\right\},$$

$$u_{n+1} = N^2 L_{yy}^{-1}(u_n),\ n \geq 0. \tag{33}$$

Following the equation (33), we get

$$u_1 = C_5 \frac{(Ny)^2}{2!} + \frac{C_6}{N}\frac{(Ny)^3}{3!} + \frac{A_0}{N^2}\frac{\partial p}{\partial x}\left\{\frac{(Ny)^4}{4!}\right\} - \frac{B_0 N^2}{A^4 F_1}\left(SinhAy + CoshAy\right) + \frac{B_0 F_0}{N^2 F_1}\left\{\frac{(Ny)^4}{4!}\right\}$$
$$- \frac{C_0 N_t F_0}{N_b N^2 F_1}\left\{\frac{(Ny)^4}{4!}\right\} + \frac{C_0 N_t N^2}{N_b A^4 F_1}\left(SinhAy + CoshAy\right) - \frac{C_0(N_t + N_b)}{N_b N^3 (h_2 - h_1)}\left\{\frac{(Ny)^5}{5!}\right\}$$
$$+ \frac{C_0(N_t + N_b)h_1}{N_b N^2 (h_2 - h_1)}\left\{\frac{(Ny)^4}{4!}\right\},$$

$$u_2 = C_5 \frac{(Ny)^4}{4!} + \frac{C_6}{N}\frac{(Ny)^5}{5!} + \frac{A_0}{N^2}\frac{\partial p}{\partial x}\left\{\frac{(Ny)^6}{6!}\right\} - \frac{B_0 N^4}{A^6 F_1}\left(SinhAy + CoshAy\right) + \frac{B_0 F_0}{N^2 F_1}\left\{\frac{(Ny)^6}{6!}\right\}$$
$$- \frac{C_0 N_t F_0}{N_b N^2 F_1}\left\{\frac{(Ny)^6}{6!}\right\} + \frac{C_0 N_t N^4}{N_b A^6 F_1}\left(SinhAy + CoshAy\right) - \frac{C_0(N_t + N_b)}{N_b N^3 (h_2 - h_1)}\left\{\frac{(Ny)^7}{7!}\right\}$$
$$+ \frac{C_0(N_t + N_b)h_1}{N_b N^2 (h_2 - h_1)}\left\{\frac{(Ny)^6}{6!}\right\},$$

$$u_3 = C_5 \frac{(Ny)^6}{6!} + \frac{C_6}{N}\frac{(Ny)^7}{7!} + \frac{A_0}{N^2}\frac{\partial p}{\partial x}\left\{\frac{(Ny)^8}{8!}\right\} - \frac{B_0 N^6}{A^8 F_1}\left(SinhAy + CoshAy\right) + \frac{B_0 F_0}{N^2 F_1}\left\{\frac{(Ny)^8}{8!}\right\}$$
$$- \frac{C_0 N_t F_0}{N_b N^2 F_1}\left\{\frac{(Ny)^8}{8!}\right\} + \frac{C_0 N_t N^6}{N_b A^8 F_1}\left(SinhAy + CoshAy\right) - \frac{C_0(N_t + N_b)}{N_b N^3 (h_2 - h_1)}\left\{\frac{(Ny)^9}{9!}\right\}$$
$$+ \frac{C_0(N_t + N_b)h_1}{N_b N^2 (h_2 - h_1)}\left\{\frac{(Ny)^8}{8!}\right\},$$

$$u_n = C_5 \frac{(Ny)^{2n}}{2n!} + \frac{C_6}{N}\frac{(Ny)^{2n+1}}{(2n+1)!} + \frac{A_0}{N^2}\frac{\partial p}{\partial x}\left\{\frac{(Ny)^{2n}}{2n!}\right\} - \frac{B_0 N^{2n}}{A^{2n+2} F_1}\left(SinhAy + CoshAy\right) + \frac{B_0 F_0}{N^2 F_1}\left\{\frac{(Ny)^{2n}}{2n!}\right\}$$
$$- \frac{C_0 N_t F_0}{N_b N^2 F_1}\left\{\frac{(Ny)^{2n}}{2n!}\right\} + \frac{C_0 N_t N^{2n}}{N_b A^{2n+2} F_1}\left(SinhAy + CoshAy\right) - \frac{C_0(N_t + N_b)}{N_b N^3 (h_2 - h_1)}\left\{\frac{(Ny)^{2n+1}}{(2n+1)!}\right\}$$
$$+ \frac{C_0(N_t + N_b)h_1}{N_b N^2 (h_2 - h_1)}\left\{\frac{(Ny)^{2n}}{2n!}\right\},$$

By the method of Decomposition by Adomian we get

$$u = \sum_{n=0}^{\infty} u_n. \tag{34}$$

Solution in closed form can be written as

$$u = C_5 CoshNy + \frac{C_6}{N} SinhNy + \frac{A_0}{N^2}\frac{\partial p}{\partial x}\{CoshNy - 1\} - \frac{B_0\left(SinhAy + CoshAy\right)}{(A^2 - N^2)F_1} + \frac{B_0 F_0\{CoshNy - 1\}}{N^2 F_1}$$
$$- \frac{C_0 N_t F_0\{CoshNy - 1\}}{N_b N^2 F_1} + \frac{C_0 N_t\left(SinhAy + CoshAy\right)}{N_b (A^2 - N^2)F_1} - \frac{C_0(N_t + N_b)\{SinhNy - Ny\}}{N_b N^3 (h_2 - h_1)} \quad (35)$$
$$+ \frac{C_0(N_t + N_b)h_1\{CoshNy - 1\}}{N_b N^2 (h_2 - h_1)}.$$

The volume flow rate is given as

$$q = \int_{h_1}^{h_2} u\, dy \quad (36)$$

The instantaneous flux at any axial is given by

$$\overline{Q}(x,t) = \int_{h_1}^{h_2} (1+u)\, dy = h_2 - h_1 + q. \quad (37)$$

The mean volume rate of flow over one period $T = \frac{\lambda}{c}$ of the peristaltic wave is

$$Q = \int_0^1 \overline{Q}\, dt = \int_0^1 (h_2 - h_1) + q\, dt = d + 1 + q. \quad (38)$$

From equation (19), the expression for pressure gradient is,

$$\frac{\partial p}{\partial x} = \left(1 + \frac{1}{\beta}\right)\frac{\partial^2 u}{\partial y^2} - \frac{M^2}{1+m^2}u + G_r\theta + B_r\Omega, \quad (39)$$

Table 1. Illustrates comparison of output of present study correlating with previous work for variations in Brownian motion term N_b and thermophoresis term N_t on temperature and concentration fields for $a = 0.1, b = 0.2, d = 1, \beta = 0.1, \varphi = 0.6, Rd = 0.3, \Pr = 6.7.$ & $b = 0.2, d = 0.5, a = 0.1, x = \varphi = 0, Rd = 0.2, \Pr = 0.1.$ respectively.

$N_t = N_b$	$\theta(x,y)$ Beg and Tripathi [30]	$\theta(x,y)$ Present work	$\Omega(x,y)$ Beg and Tripathi [30]	$\Omega(x,y)$ Present work
1	0.9845	0.9764	0.8715	0.8579
2	0.9942	0.9828	0.8125	0.8020
3	1.0024	0.9971	0.7261	0.7037

We compared the present work with the results obtained by Beg et. al [30]. We can see that the good agreement between the results as shown in Table 1.

4. DISCUSSION OF RESULTS

In this section the influence of various parameters on Casson nano fluid are elaborated in detail with the aid of graphs. The pertinent parameters of significant interest comprises Hall effect m, radiation parameter Rd Brownian motion term N_b, thermophoresis term N_t, Hartmann number M, Casson fluid term β, Grashof number G_r.

4. 1. Velocity profile

Figures (2) to (4) are demonstrated to analyse the impacts of Casson fluid parameter β, local temperature Grashof number G_r, hall effect m on velocity profile. These velocity profiles exhibit the shape of parabola. Figure (2) depicts that velocity profile enhances with increase in fluid parameter β. Physically speaking, fluid parameter enhances the viscous forces and these forces have tendency to reduce the thermal boundary layer. Figure (3) illustrates that increasing Grashof number impacts the axial velocity to enhance further, due to the fact that raise in local Grashof number increases the buoyancy force and this in turn affects axial velocity to increase. Figure (4) shows that axial velocity profile diminishes with increase in uniform parameter m particularly in the middle portion of the channel.

4. 2. Temperature Distribution

Figures (5) to (7) include variations of temperature field for different parameters such as Brownian motion term (N_b), thermophoresis term (N_t) and Radiation term (Rd). Figure (5) shows the impact of term Brownian motion N_b on temperature field. It is noticed that increase in the value of N_b enhances the temperature. Similar behaviour can be drawn from Figure (6) for thermophoresis parameter (N_t) wherein temperature profile enhances with the raise in N_t. Figure (7) depicts the variations of temperature with an effect of thermal radiation parameter (Rd). We have seen that distribution of temperature declines with the raise in radiation parameter.

4. 3. Nanoparticle Concentration

Figures (8) to (10) describes the variations of concentration profile for different parameters like thermophoresis, Brownian motion and radiation terms. In Figure (8) and Figure (9) we have shown the impact of thermophoresis term and Brownian motion term on concentration profile. It is observed in both shows equivalent behaviour on concentration distribution in which nanoparticles concentration diminishes slowly with N_t and N_b. While raise in thermophoresis term enhances the temperature profile. Figure (10) depicts the variation in concentration profile regarding radiation parameter. It is seen that concentration profile enhances with the raise in radiation term Rd.

4. 4. Pressure gradient

Figures (11) to (13) illustrates the behaviour of pressure gradient $\frac{dp}{dx}$ with respect to parameters like Hall current (m), Hartmann number (M) and radiation parameter (Rd). In figure (11) we have demonstrated the effect of Hall current on gradient of pressure. It is clear from the graph that pressure gradient $\frac{dp}{dx}$ decreases with increase in Hall effect term (m) in such a way that rising the Hall parameter increases the pressure gradient in the middle of the channel thus not allowing the fluid to flow easily in the mid of the region. Figure (12) shows the effect of Hartmann number (M) on the distribution of pressure gradient. One can see that graph shows opposite behaviour when compared to hall current (m), wherein increasing the pressure gradient inside the fluid flow which in turn does not allow the fluid to pass easily through the channel. Figure (13) depicts the relation between pressure gradient $\frac{dp}{dx}$ and radiation parameter (Rd). We have observed that increase in radiation parameter diminishes the pressure gradient of the fluid motion. It is also examined that both Hall and Radiation term depicts the similar nature on the fluid motion.

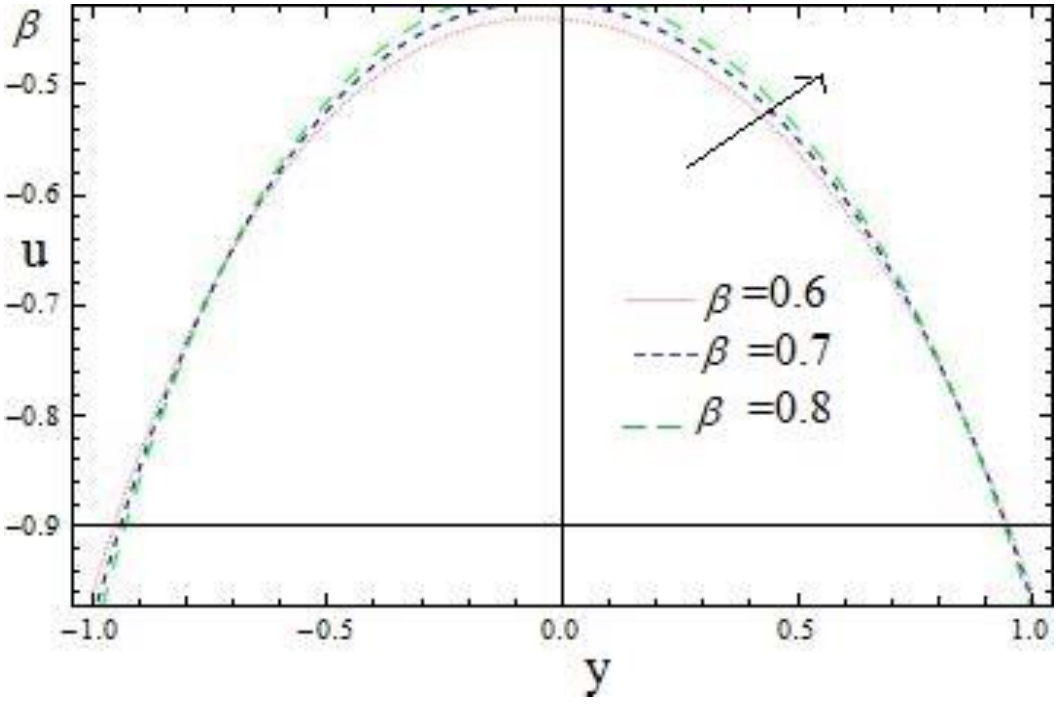

Figure 2. The velocity field versus y for different Casson fluid parameter $a = 0.1,\ b = 0.5,\ d = 0.7,\ x = 0.1, \varphi = 0.2,\ dp/dx = 3, \Pr = 6.7, M = 3.$

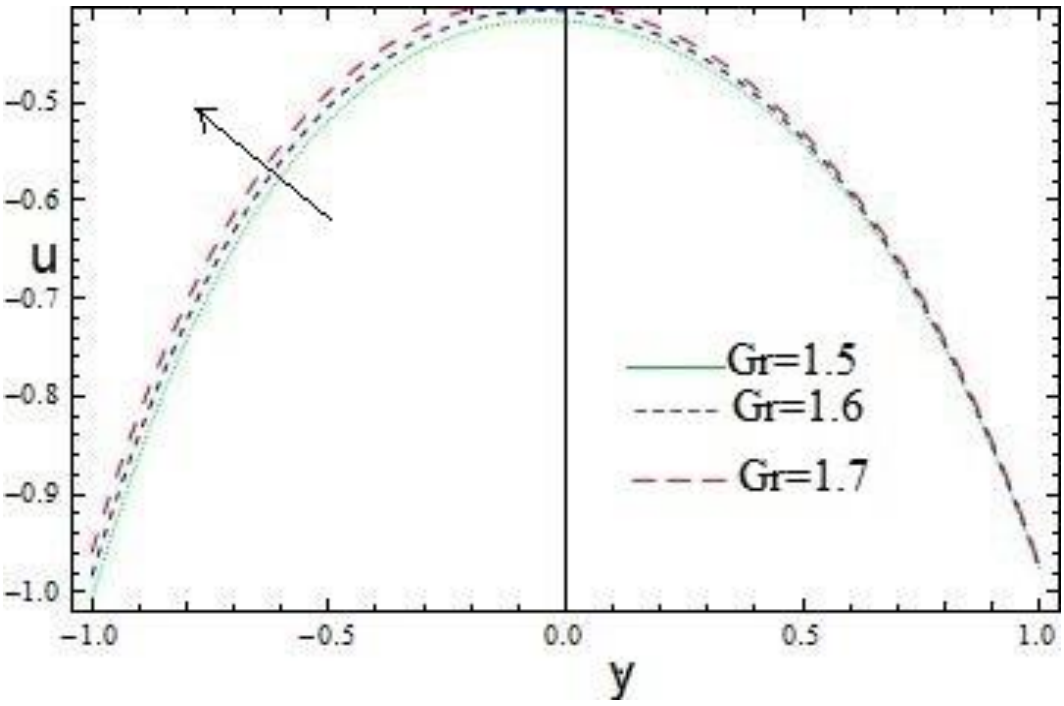

Figure 3. The velocity field versus y for different Grashof number when $Rd = 0.5, Br = 0.5, m = 0.1, N_t = 1.6, N_b = 0.6, \beta = 0.8.$

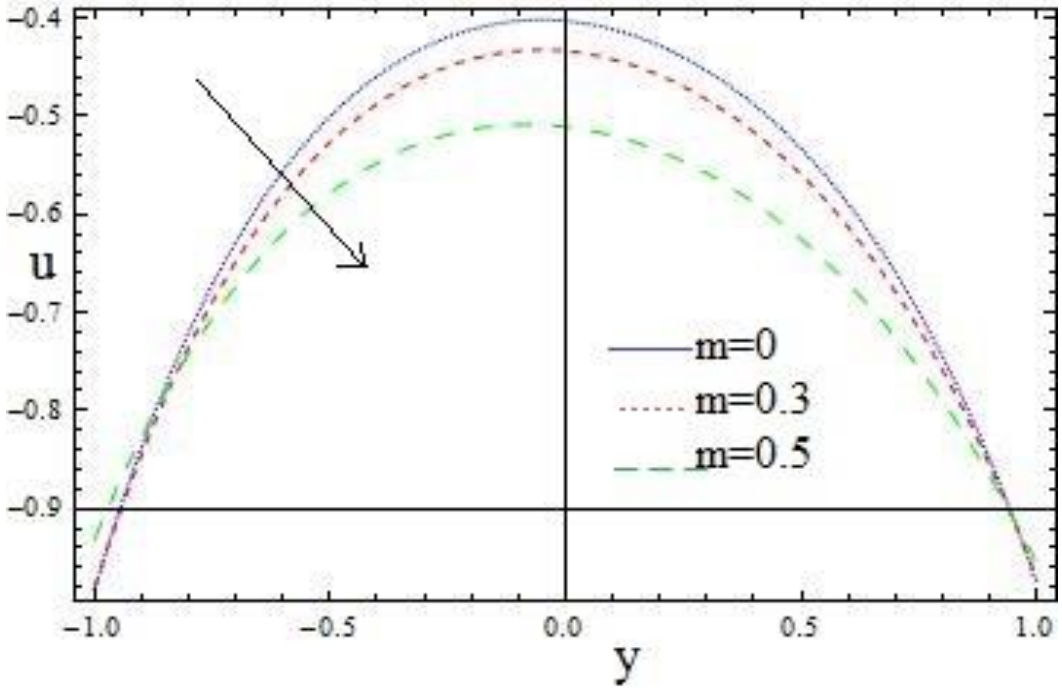

Figure 4. The velocity field versus y for different Hall parameter when $\beta = 0.8, Rd = 0.5, N_t = 1.6, N_b = 0.6, Br = 0.5, Gr = 1.6.$

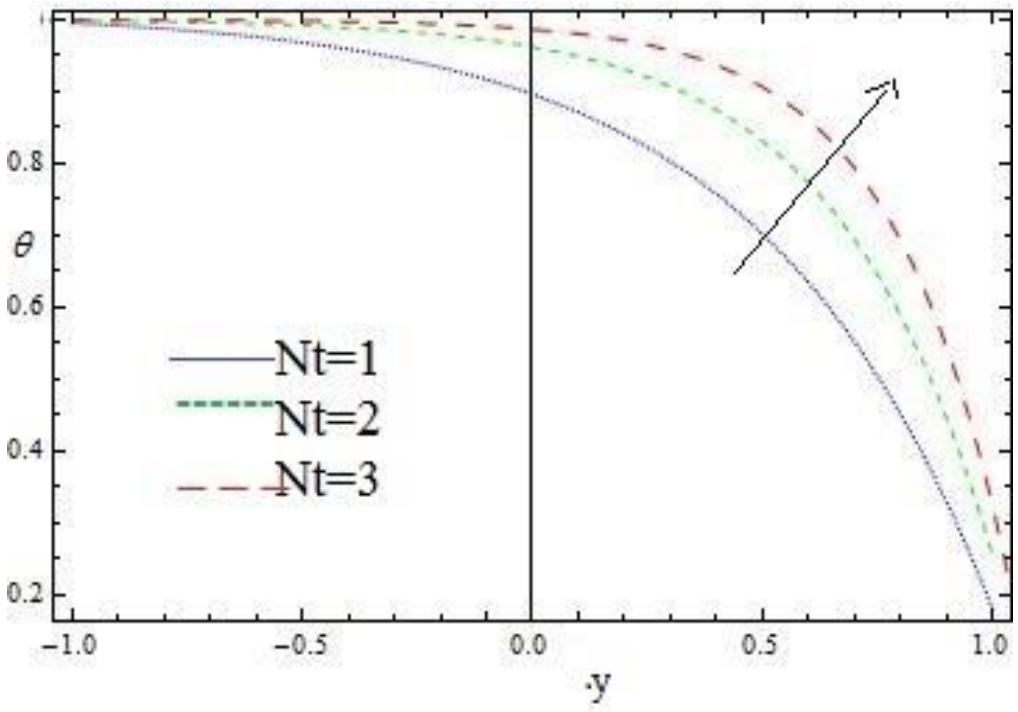

Figure 5. The temperture θ versus y for different values of (N_t)
$x = 0.1, a = 0.1, b = 0.2, d = 1, \varphi = 0.6, \beta = 0.1, \Pr = 6.7.$

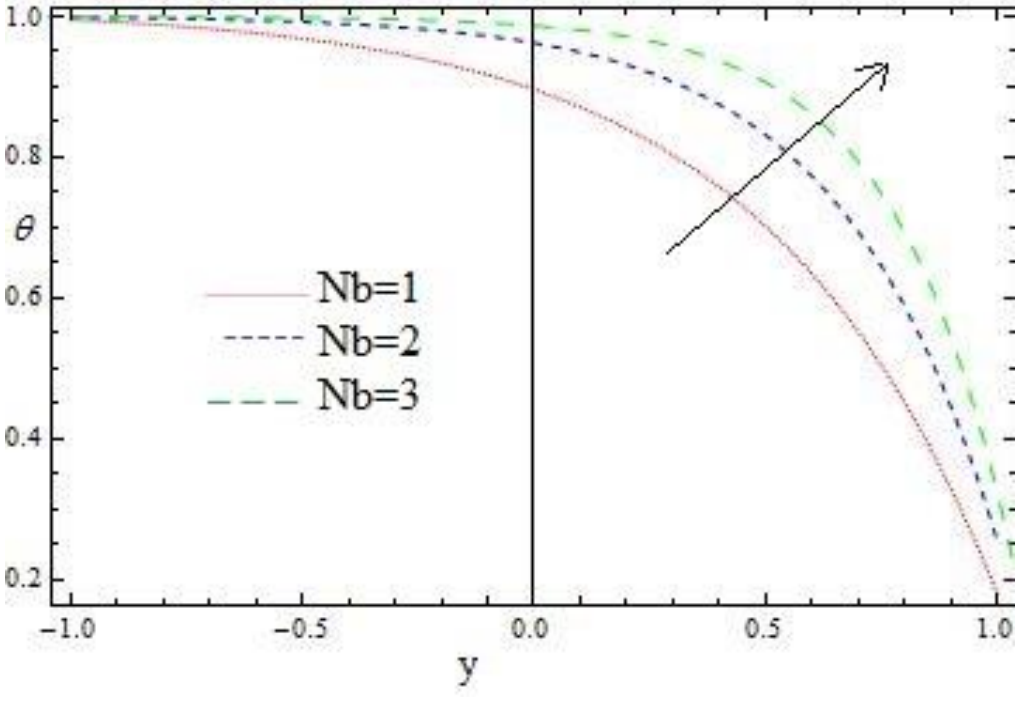

Figure 6. The temperture θ versus y for different values of (N_b)
$N_t = 1, Rd = 0.3.\ \ b = 0.2, d = 1, \varphi = 0.6, \beta = 0.1, \Pr = 6.7.$

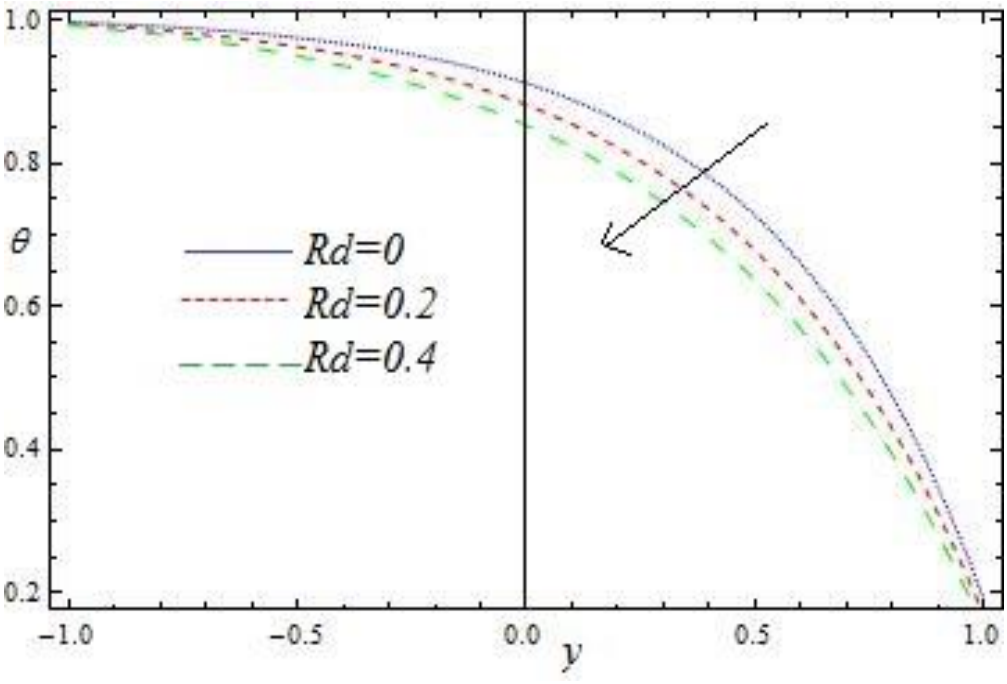

Figure 7. The temperture θ versus y for different values of (Rd) when $N_t = N_b = 3, b = 0.2, d = 1, \varphi = 0.6, \beta = 0.2, \Pr = 0.8$

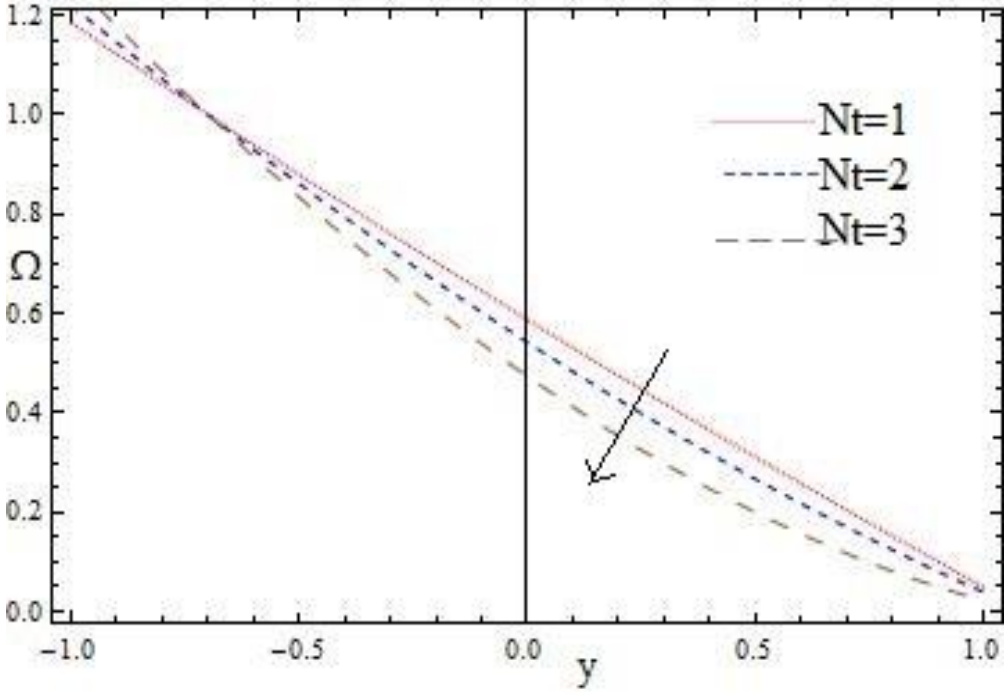

Figure 8. Concentration distribution Ω versus y for different values of (N_t) $Pr = 0.7,\ \phi = 0.7, x = 0.1;$

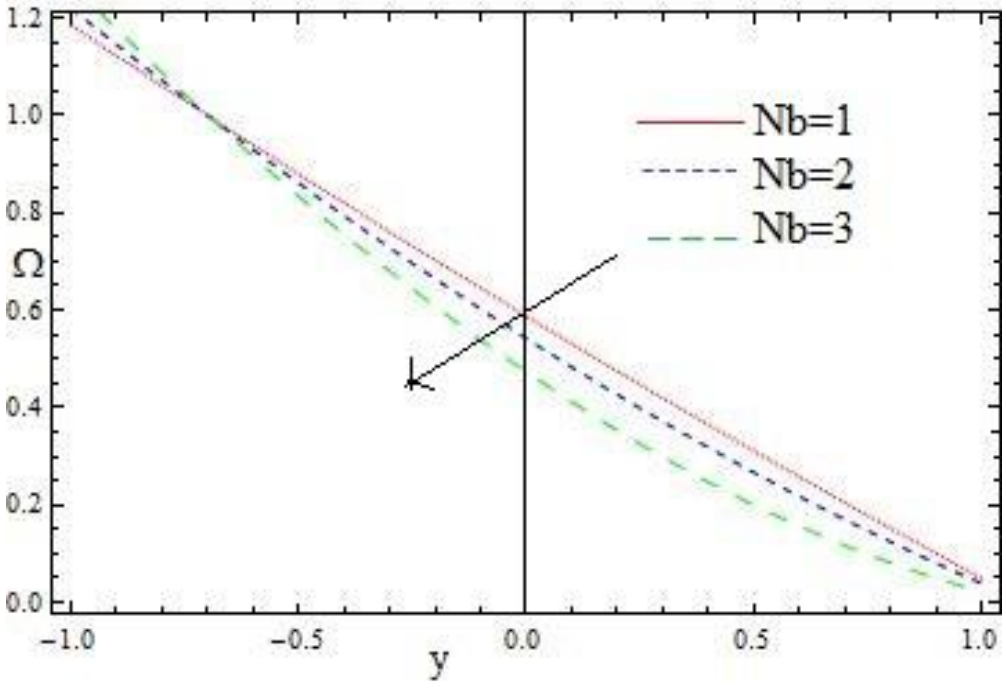

Figure 9. Concentration distribution Ω versus y for different values of (N_b) when $N_b = 0.9, Rd = 0.5.$

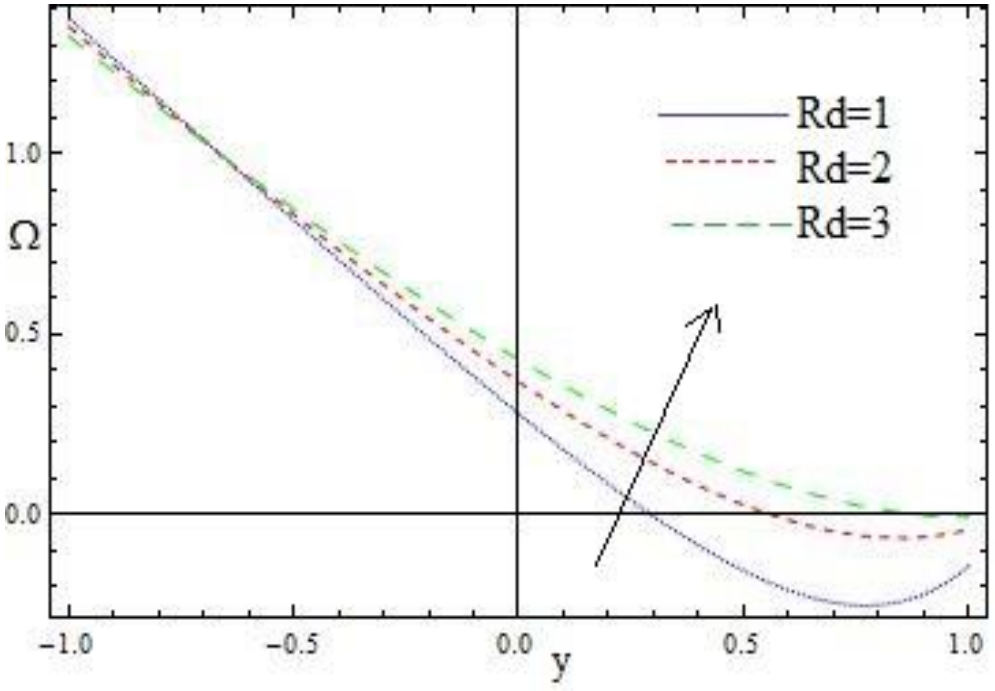

Figure 10. Concentration distribution Ω versus y different values of (Rd) when $N_t = N_b = 0.5.$

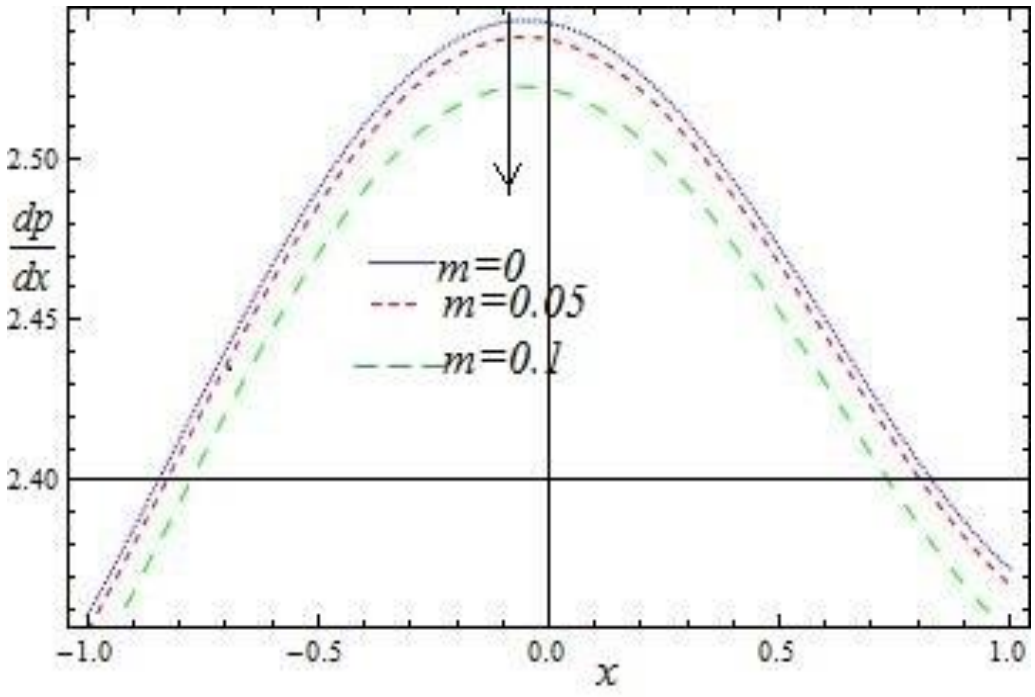

Figure 11. Pressure gradient $\frac{dp}{dx}$ versus x for different Hall parameter for $N_t = N_b = 1, Pr = 6.7, Gr = Br = 0.6, \beta = 0.5, \phi = 0.1, a = 0.1, b = 0.5, d = 0.7, q = 0.1.$

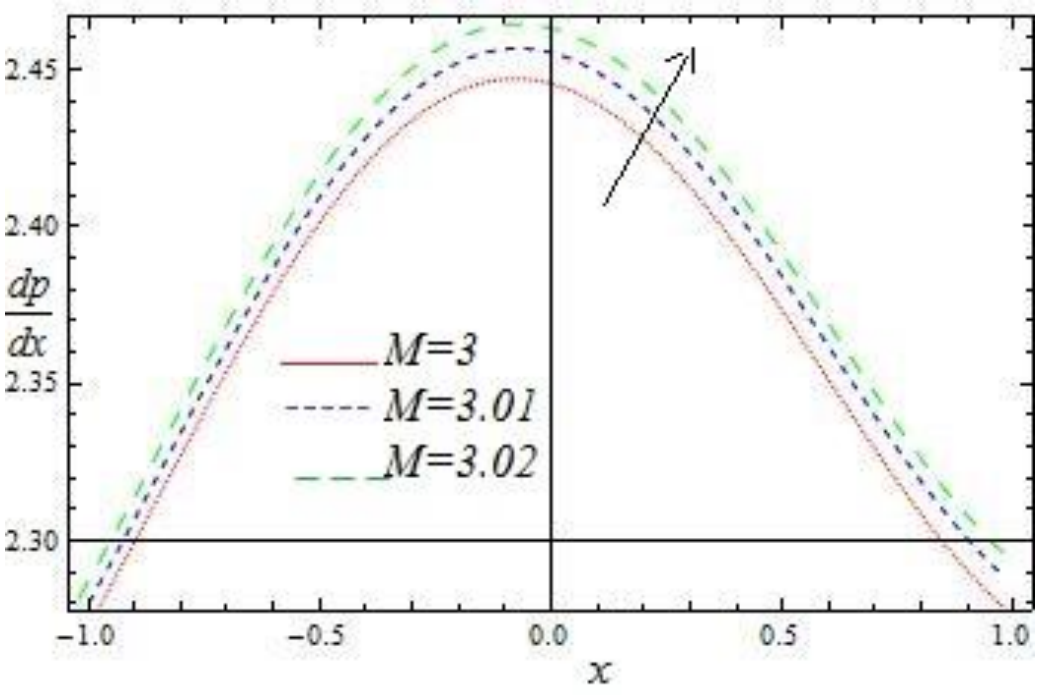

Figure 12. Pressure gradient $\frac{dp}{dx}$ versus x for different Magnetic parameter $m = 0.2, Rd = 0.1, x = 0.2.$

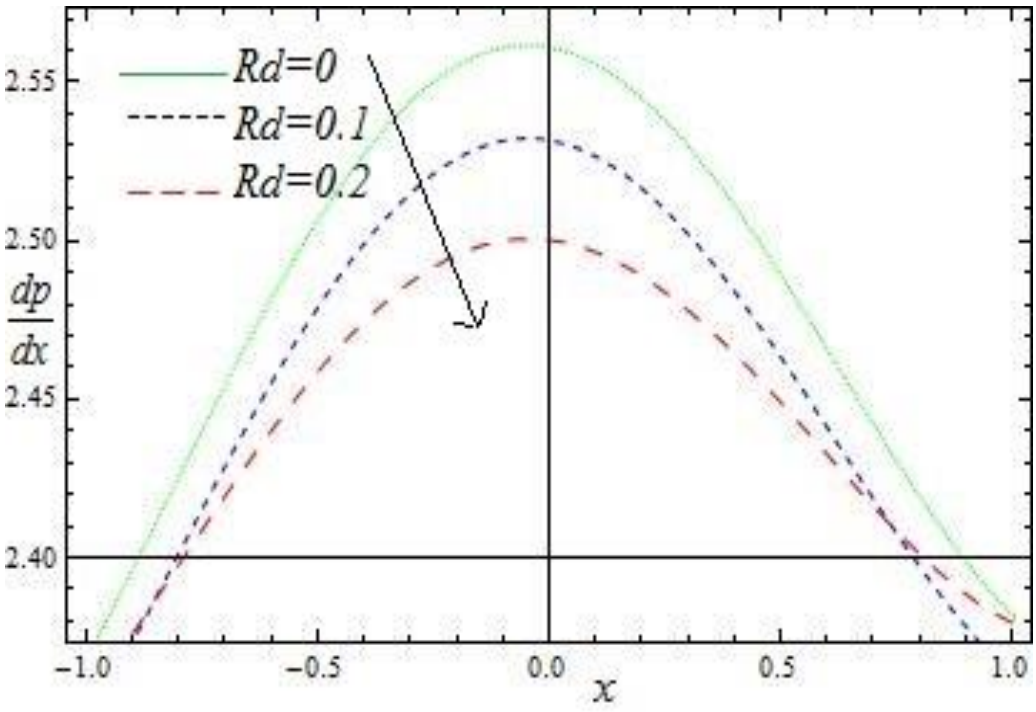

Figure 13. Pressure gradient $\frac{dp}{dx}$ versus x for fixed values of Rd when $m = 0.1, M = 3, x = 0.$

5. CONCLUDING REMARKS

The flow of perstaltic Casson nano fluid under the combined effects of thermal radiation and hall current have been studied analytically with the help of MATHEMATICA software. The pressure gradient, temperature and concentration profiles are plotted for the different flow parameters. The vital findings of this study have a scope in branches like thermotherapy, chemotherapy and novel drug delivery systems.

We can summarize the key points as below.

- The local thermal Grashof number has enhancing effect on the axial velocity profile.
- The velocity field enhances with a raise in hall parameter near the channel walls perhaps velocity profile diminishes at the middle portion of the channel.
- It is observed that all three parameters Thermal radiation Rd , Thermophoresis N_t and Brownian motion N_b have diminishing effects on the temperature θ .
- Analysed from the graphs that Radiation term Rd diminishes the temperature but enhances the concentration and pressure gradient of the flow.
- Both Hall current (m) and Radiation parameter (Rd) have the opposite behaviour on pressure gradient profile.

Nomenclature

$(\bar{X},\bar{Y})$ lab frame
$(\bar{x},\bar{y})$ wave frame
Q volume rate of flow in lab frame
$(\bar{U},\bar{V})$ components of velocity in lab frame
C_1, C_0 wall concentration
(u,v) velocity components in wave frame
c wave speed
a_1, a_2 lower wall amplitudes
$d_2 + d_1$ channel width
h_1 upper wall
h_2 lower wall
g free fall acceleration
p fluid pressure in wave frame
P fluid pressure in lab frame
q flux in the wave frame
t time
C_p specific heat at constant pressure
e_{ij} $(i,j)^{th}$ component of rate of deformation
B_0 strength of the applied magnetic field
C Concentration
M Hartmann number
ρ_y yield stress of the fluid
K_1 permeability parameter
Sc Schmidt number
G_r Grashof number
R' chemical reaction term
k_1 rate of chemical reaction

Greek symbols

β heat generation parameter
λ wavelength
ϕ phase difference
π_c a critical value of π
γ casson fluid parameter
δ wave number
ρ density

References

[1] J.C. Maxwell, A treative on electricity and magnetism. Dover Publications. 1873.

[2] S.U.S. Choi, Development and applications of non-Newtonian flows. *ASME Fluids Engineering Divion* 66 (1995) 99-106

[3] S.U.S. Choi and J.A. Eastman, Enhancing thermal conductivity of fluids with nano-particles. *ASME Fluids Engineering Divion* 231 (1995) 99-105

[4] P. Vassalo, R. Kumar and S. D'Amico, Pool boiling heat tranfer expriements in silica – water nanofluids. *Intranational Journal of Heat mass transfer* 47 (2004) 407-411

[5] S.M.You, J.H. Kim and K.H. Kim, Effect of nanoparticles on critical heat flux of water in pool boiling heat transfer. *Applied Physics Letter* 83 (2003) 3374-3376

[6] T. Hayat, B. Ahmed, F.M. Abbasi and A. Alsaedi, Numerical investigation for peristaltic flow of Carreau-yasuda magneto-nanofluid with modified darey and radiations. *Journal of Thermal Analysis and Calorimetry* 137 (2019) 1-9

[7] Sadia Ayub, T. Hayat, S. Asghar and B. Ahmed, Thermal radiation impact in mixed convective peristaltic flow of third grade nanofluid. *Results in Physics* 7 (2017) 3687-3695

[8] A.S. Kotnurkar, S. Giddaiah, Peristaltic transport of Eyring powell nanofluid in a non-unifrom channel. *Jordan Journal of Mathematics and Statstics* 12 (2019) 134-138

[9] A.S. Kotnurkar, S. Giddaiah, Bioconvection peristaltic transport of nanofluid in a channel containing gyrotactic microorganism. *Journal of Informatics and Computing Science* 14 (2019) 134-148

[10] K. Ahmed, R. Nazar, Magnetohydrodynamic three-dimensional flow and heat transfer over a stretching surface in a visco-elastic fluid. *Journal of Science and Technology* 3(1) (2011) 33-46

[11] S. Nadeem, R.U. Haq and C. Lee, MHD flow of a Casson fluid over an exponentially shrinking sheet. *Scientia Iranica* 19 (2012) 1550-1553

[12] A. Ebaid, Effects of magnetic field and wall slip conditions on the peristaltic transport of Newtonian fluid in an asymmetric channel. *Physics Letters A*.372 (2008) 4493-4499

[13] S. Nadeem, S. Akram, Slip effects on the peristaltic flow of Jeffrey fluid in an asymmetric channel under the effect of induced magnetic field. *International Journal for Numerical Methods in Fluids* 63 (2010) 374-394

[14] Kh. S. Mekheimer, Y. Abd Elmaboud, The influence of heat transfer and magnetic field on peristaltic transport of a Newtonian fluid in a vertical annulus: Application of an endoscope. *Physics Letters A*. 372 (2008) 1657-1665

[15] S. K. Asha and K. Deepa, Peristaltic flow of a third grade fluid accounting Joule heating Magnetic field effects in an asymmetric channel. *World Scientific News* 137 (2019) 1-17

[16] L. M. Srivastava, V.P. Srivastava, Peristaltic transport of blood: Casson Model II, *Journal of Biomechanics* 17 (1984) 821-829

[17] A.V. Mernone, J.N. Mazumdar, A mathematical study of peristaltic transport of Casson fluid. *Mathematical and Computer Modelling* 35 (2002) 894-912

[18] Balamurugan KS, Prakash J, Varma SV. Effects of thermo and chemical reaction on three dimensional MHD free convection flow of couette. *WJ Science and Technology* 12 (9) (2014) 805-830

[19] Muhammad Mubashir Bhatti, Munawwar Ali Abbas and Mohammad Mehdi Rashidi, Entropy generation for Peristaltic blood flow with Casson Model and consideration of magnetohydrodynamics effects. *Walailak Journal of Science and Technology* 14 (6) (2017) 451-461

[20] P. Nagarani, G. Sarojamma, Peristalic transport of Casson fluid in an asymmetric channel. *Australasian Physics & Engineering Science in Medicine* 27 (2004) 49-59

[21] P. Nagarani, Peristaltic transport of a Casson fluid in an inclined channel. *Korea-Australia Rheology Journal* 22 (2010) 105-111

[22] S. Nadeem, R.U.Haq and C. Lee, MHD flow of a Casson fluid over an exponentially shrinking sheet. *Scientia Iranica* 19 (2012) 1550-1553

[23] L. M. Srivastava, Peristaltic transport of Casson fluid. *Nigeria Journal Science and Results* 1 (1987) 71-82

[24] T. Hayat, M. Rashidi, M. Imtiaz and A. Alsaedi, MHD convective flow due to a curved surface with thermical radiation and chemical reaction. *Journal of Molecular Liquid* 225 (2017) 482-489

[25] J. Tawadi, M. S. Abel, P. G. Metri and A. Koti, Thin film flow and heat transfer over an unsteady stretching sheet with thermal radiation, internal heating in the presence of external magnetic field, *International Journal of Advances in Applied Mathematics and Mechanics* 3 (4) (2016) 29-40

[26] M. I. Khan, Q. M.zaigham, A. Alsaedi and T. Hayat, Thermally stratified flow of second grade fluid with non-Fourier heat flux and temperature dependent thermal conductivity. *Results in Physics* 8 (2018) 799-804

[27] A.M. Hussain, K. Khanafer and K.Vafai, The effect of radiation on free convection flow of fluid with variable viscosity from a porous vertical plate. *International Journal of Thermal Science* 40 (2) (2001) 115-121

[28] S. Rosseland, Astrophysik und atom-theoretische Grundlagen. Springer Verlag, Berlin, 1931, pp. 41-44

[29] A. Bharali, and A. K. Borkakati, The effect of hall currents on MHD flow and heat transfer between two parallel porous plates. *Applied Sciences Results* 39 (2) (1982) 155-165

[30] O.A. Beg and D. Tripathi, A study on peristaltic flow of nanofluids: Application in drug delivery systems. *International Journal of Heat and Mass Transfer* 70 (2014) 61-70

Appendix A: Supplementary data

$$C_1 = \frac{N_t + N_b}{N_b(h_2 - h_1)},\quad C_2 = \frac{(N_t + N_b)h_1}{N_b(h_1 - h_2)},\ C_3 = \frac{1 - F_0}{F_1},\qquad C_4 = \frac{A}{F_1},$$

$$C_5 = \frac{A_0 dp/dx(SinhNh_2 - SinhNh_1 - SinhN(h_2 - h_1))}{N^2 SinhN(h_2 - h_1)} + \frac{(2CoshNh_1 - 1)(SinhNh_2 - SinhNh_1)}{SinhN(h_2 - h_1)}$$
$$\left(\frac{C_0 N_t F_0}{N_b F_1 N^2} - \frac{C_0(N_t + N_b)h_1}{N_b(h_2 - h_1)N^2} - \frac{B_0 F_0}{N^2 F_1}\right) + \left(\frac{\left(F_0\left(CoshNh_1 - CoshNh_2\right) - F_1 CoshNh_1\right)(SinhNh_2 - SinhNh_1)\left(B_0 N_b - C_0 N_t\right)}{(CoshNh_1 - CoshNh_2)N_b F_1 SinhN(h_2 - h_1)(A^2 - N^2)}\right) +$$
$$\left(\frac{C_0(SinhNh_2 - SinhNh_1)(N_t + N_b)\left(\left(Sinh2Nh_1 - SinhN(h_2 + h_1) - 2Nh_1 CoshNh_1 + N(h_1 CoshNh_2 + h_2 CoshNh_1)\right)\right)}{(CoshNh_1 - CoshNh_2)N_b SinhN(h_2 - h_1)N^3(h_2 - h_1)}\right)$$
$$+ \frac{B_0}{(A^2 - N^2)(CoshNh_1 - CoshNh_2)} + \frac{B_0 F_0}{N^2 F_1} - \frac{C_0 N_t F_0}{N_0 F_1 N^2} - \frac{C_0 N_t}{N_0(A^2 - N^2)(CoshNh_1 - CoshNh_2)} -$$
$$\left(\frac{C_0((SinhNh_1 - SinhNh_2 - N(h_1 - h_2))(N_t + N_b)}{(CoshNh_1 - CoshNh_2)N_b SinhN(h_2 - h_1)N^3(h_2 - h_1)}\right) + \frac{C_0 h_1(N_t + N_b)}{N_b(h_2 - h_1)N^2} - \frac{(SinhNh_2 - SinhNh_1)}{SinhN(h_2 - h_1)},$$

$$C_6 = \frac{A_0 dp/dx(C\,\mathrm{os}\,hNh_1 - CoshNh_2)}{NSinhN(h_2 - h_1)} + \frac{(2CoshNh_1 - 1)N(CoshNh_1 - CoshNh_2)}{SinhN(h_2 - h_1)}$$
$$\left(\frac{C_0 N_t F_0}{N_b F_1 N^2} - \frac{C_0(N_t + N_b)h_1}{N_b(h_2 - h_1)N^2} - \frac{B_0 F_0}{N^2 F_1}\right) + \left(\frac{N\left(F_0\left(CoshNh_1 - CoshNh_2\right) - F_1 CoshNh_1\right)\left(B_0 N_b - C_0 N_t\right)}{N_b F_1 SinhN(h_2 - h_1)(A^2 - N^2)}\right) +$$
$$\left(\frac{C_0(N_t + N_b)\left(\left(Sinh2Nh_1 - SinhN(h_2 + h_1) - 2Nh_1 CoshNh_1 + N(h_1 CoshNh_2 + h_2 CoshNh_1)\right)\right)}{N_b SinhN(h_2 - h_1)N^2(h_2 - h_1)}\right) -$$

$$\frac{N(CoshNh_1 - CoshNh_2)}{SinhN(h_2 - h_1)},$$

$$F_0 = SinhAh_1 + CoshAh_1,$$
$$F_1 = (SinhAh_2 + CoshAh_2) - (SinhAh_1 + CoshAh_1),$$
$$A = \frac{(N_t + N_b)\,\mathrm{Pr}}{(1 + Rd\,\mathrm{Pr})(h_1 - h_2)},$$
$$N = \sqrt{\frac{M^2\beta}{(1 + m^2)(1 + \beta)}},$$
$$A_0 = \frac{\beta}{(1 + \beta)},$$
$$B_0 = \frac{Gr\beta}{(1 + \beta)},$$
$$C_0 = \frac{Br\beta}{(1 + \beta)},$$